JOURNAL OF RAMAN SPECTROSCOPY, VOL. 17, 437–446 (1986)

The Conformational Equilibria and the IR and Raman Spectra of 2-(Choromethyl)-2-methyl-1,3-dichloropropane

K. Martinsen, D. L. Powell†, C. J. Nielsen and P. Klaeboe*
Department of Chemistry, University of Oslo, 0315 Oslo 3, Norway

The infrared spectra of 2-chloromethyl-2-methyl-1,3-dichloropropane in several phases, including the pure liquid, as a solute and as an amorphous and crystalline solid at 80 K and under pressure (2–30 kbar), have been recorded. Raman spectra of the neat liquid and of the plastic and anisotropic crystalline phases were obtained at various temperatures.

A large number of IR and Raman bands present in the neat liquid, in solution and in the plastic crystalline phase vanished in the low-temperature and in the high-pressure crystal spectra. Among seven possible conformers, three (having symmetries C_1, C_s and C_3) have no 1,3-parallel C—Cl bonds and are present in the liquid, in solution and in the plastic phase. In the anisotropic crystal, only the C_1 conformer was present. A phase transition between the plastic and anisotropic crystal occurred at 253 K. ΔH^0 values between the most stable conformers C_s and C_1 were 5 ± 1 and 3 ± 1 kJ mol^{-1} K^{-1} in the plastic phase and in the liquid phase, respectively.

A force constant calculation for the C_1, C_s and C_3 conformers and for various conformers of other halogenated neopentanes (a total of 11 conformer molecules) was carried out with the overlay technique. A 41-parameter force field was adjusted to more than 280 observed frequencies, giving very satisfactory agreement.

The spectra were interpreted in terms of conformers of C_1, C_s and C_3 symmetry.

INTRODUCTION

We have been interested for a long time in the structure and conformations of halogenated propanes and a number of 1,2-dihalo-, 1,3-dihalo- and 1,2,3-trihalo-propanes have been studied.[1] Neopentane (2,2-dimethylpropane), with a pronounced spherical shape, represents an interesting derivative of propane and is known to form a plastic phase.[2] The halogenated neopentanes have various possible conformers, of which a few are abundant in the vapour[3] and in the liquid states. The vibrational spectra of some halogenated neopentanes have recently been recorded in our laboratory with special emphasis on spectral changes between the liquid and crystalline states. Our results for monochloroneopentane (1-chloro-2,2-dimethylpropane)[4] and dichloroneopentane (2,2-dimethyl-1,3-dichloropropane)[5] have been reported. In addition, we have recently completed studies of two tetrahaloneopentanes [2,2-di(chloromethyl)-1,3-dichloropropane and 2,2-di(bromomethyl)-1,3-dibromopropane].[6]

In this paper we report our results for 2-chloromethyl-2-methyl-1,3-dichloropropane (trichloroneopentane; TRCN). Very little work has been carried out on TRCN since its initial synthesis in 1952.[7] The dipole moment has been determined[8,9] and the infrared and Raman spectra reported in the 700–800 cm^{-1} range.[10] The conformational equilibria of TRCN and other halogenated neopentanes in the vapour phase were investigated by Stølevik[3,11–13] using electron diffraction and molecular mechanics calculations. He observed[11] 45% of conformer C_s, 34% of C_1 and 21% of C_3 in the vapour phase at 361 K (C_s, C_1 and C_3 refer to the point group symmetries of the TRCN conformers). The additional four conformers have two or three 1,3-diparallel C—Cl bonds and their energies are more than 16 kJ mol^{-1} higher than that of the most stable conformer as estimated from molecular mechanics calculations. Conformational studies by ^{1}H NMR spectroscopy at the coalescence temperature 102 K in $CBrF_3$ solution have given 58% C_s, 34% C_1 and 8% C_3.[14]

We also report the vibrational spectra of TRCN in the liquid state, in solution and in the plastic crystalline and anisotropic solids at low temperature and under high pressure. The Raman and IR spectra have been interpreted with the aid of normal coordinate analyses on 11 different halogenated neopentane conformers, treated by the overlay technique.

EXPERIMENTAL

TRCN was a commercial product from the K&K Laboratories which was purified by fractional distillation before use. Gas chromatographic analysis revealed the purity to be better than 99%.

Infrared spectra were recorded with a Perkin-Elmer Model 225 spectrophotometer (4000–200 cm^{-1}), a Bruker Model 114C Fourier transform spectrophotometer (3200–50 cm^{-1}) and a Hitachi FIS-1 spectrophotometer (400–100 cm^{-1}). Raman spectra were obtained on a modified Cary 81 spectrometer and on a DILOR RTI-30 (triple monochromator) which was interfaced to the Aspect 2000 data system of the Bruker FTIR. The spectra were excited by a Model 52G argon

* Author to whom correspondence should be addressed.
† On leave from The College of Wooster, Wooster, OH 44691, USA.

0377-0486/86/060437-10 $05.00

Received 4 July 1985

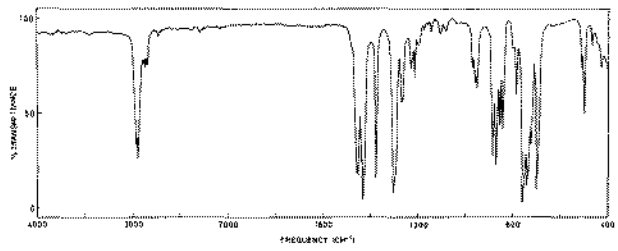

Figure 1. Mid-IR spectrum of 2-(chloromethyl)-2-methyl-1,3-dichloropropane (TRCN) as a liquid.

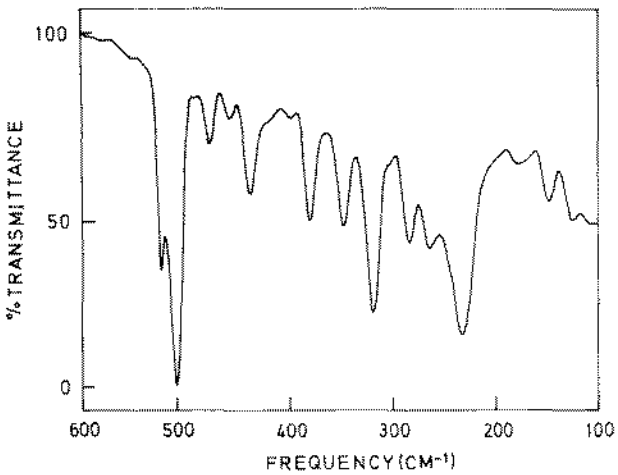

Figure 2. Far-IR spectrum of TRCN dissolved in C_6H_{12}.

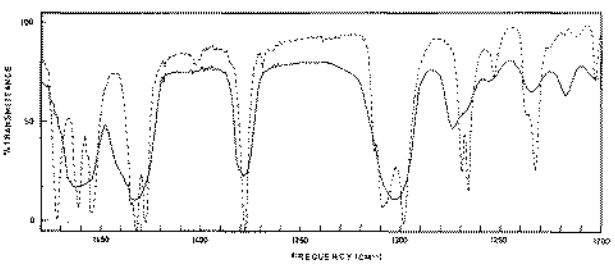

Figure 3. Mid-IR spectra of TRCN at *ca* 80 K: amorphous solid (solid curve); annealed, crystalline solid (dashed curve).

ion laser from CRL in the 90° and 180° illumination modes using the 514.5 and 488.0 nm lines.

Infrared spectra of TRCN as a neat liquid and in CCl_4, CS_2, C_6H_6 and CH_3CN solutions were recorded in sealed cells with KBr, CsI and polyethylene windows. Amorphous and crystalline samples were studied by shock-freezing the vapour on windows of CsI (4000–200 cm^{-1}) or silicon (600–50 cm^{-1}) at 80 K, and subsequent annealing to 150 K. A diamond anvil cell with type IIa diamond windows equipped with gaskets of brass, bronze or inconel with holes of 0.4 mm diameter was employed for the high-pressure studies. The sample was studied in a polarization microscope between successive recordings and the crystallization followed by visual observations. A 4× beam condenser from Perkin-Elmer was used in the Perkin-Elmer and Bruker spectrometers.

Raman spectra of TRCN was recorded at 295 and 353 K as a plastic phase. For both measurements the sample was loaded into a capillary glass tube of 2 mm

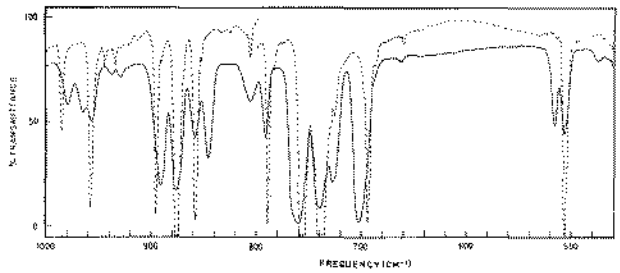

Figure 4. Mid-IR spectrum of TRCN at *ca* 80 K. Curves as in Fig. 3.

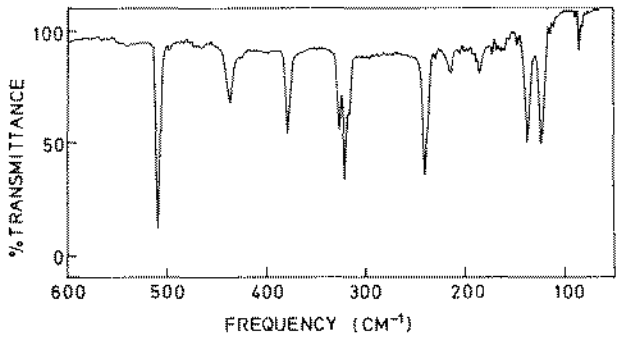

Figure 5. Far-IR spectrum of TRCN at *ca* 80 K as an annealed, crystalline solid.

i.d., placed inside a Dewar vessel[16] and heated or cooled by gaseous nitrogen. The liquid was studied by the 90° and the plastic solid by the 180° illumination mode. The anisotropic crystal was studied by cooling the plastic phase to 200 K in the same experimental set-up.[16] In separate experiments the vapour of TRCN was shock-frozen on a copper plate cooled to 80 K. The spectrum was recorded, subsequently annealed to *ca* 150 K, recooled to 80 K and a spectrum of the anisotropic crystalline solid recorded.

RESULTS AND DISCUSSION

The spectra of TRCN as a liquid in the mid-IR (4000–400 cm^{-1}) and far-IR (600–100 cm^{-1}) regions are presented in Figs 1 and 2, respectively. Selected IR curves showing the amorphous (solid line) and the annealed anisotropic crystalline solid (dotted line) at 80 K are shown in Figs 3 and 4. A far-IR crystal spectrum appears in Fig. 5. High-pressure spectra of TRCN obtained at *ca* 20 kbar showing the high-pressure anisotropic crystal are given in Figs 6, 7 and 8. A Raman spectrum of the liquid appears in Fig. 9 and the spectrum of the anisotropic crystal at 201 K in Fig. 10. The maxima of the various IR and Raman bands observed in the different phases are listed in Table 1.

High-pressure behaviour

At a very low pressure, probably at *ca* 1 kbar, a plastic crystal was formed in the diamond anvil cell at ambient temperature. Thin, wavy lines were seen to run through the solid, which was completely colourless in polarized light. The IR spectrum of this phase was nearly identical

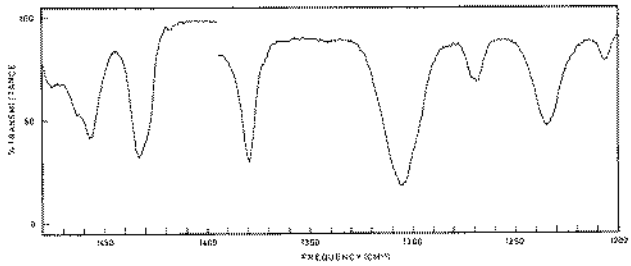

Figure 6. Mid-IR high-pressure (*ca* 20 kbar) spectrum of TRCN as an anisotropic crystal observed in a diamond anvil cell (DAC).

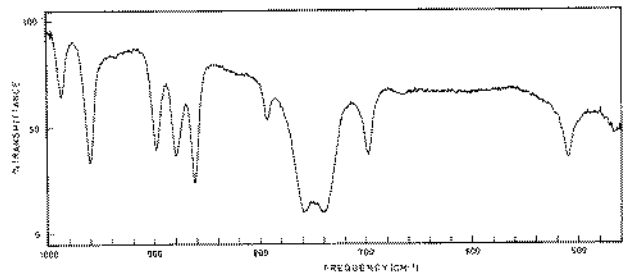

Figure 7. High-pressure IR spectrum of TRCN.

with the liquid spectrum. In particular, no IR bands present in the liquid-state spectra vanished in this solid phase, revealing that a mixture of conformers was present. These results are in perfect agreement with those obtained for other molecules which form plastic crystals,

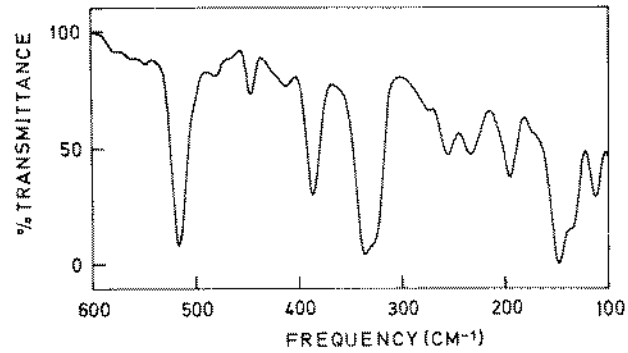

Figure 8. High-pressure far IR spectrum of TRCN.

such as succinonitrile,[17] cyclohexane monosubstituted with fluorine,[18] chlorine,[19,20] cyanide, isocyanide[21] and isocyanate[22] as substituents and 1,3-dichloro-2,2-dimethylpropane.[5] Invariably, the plastic phases in all these compounds contained a mixture of conformers similar to the vapour and the liquid states.

When the pressure of TRCN was increased to *ca* 5 kbar, however, an anisotropic crystal was formed, appearing with bright-coloured regions in a polarization microscope. The IR spectra of this phase showed that a number of bands (those marked with asterisks in Table 1) vanished. Except for the usual shift to higher wavenumbers, the spectra were unchanged up to *ca* 30 kbar (the highest pressure applied).

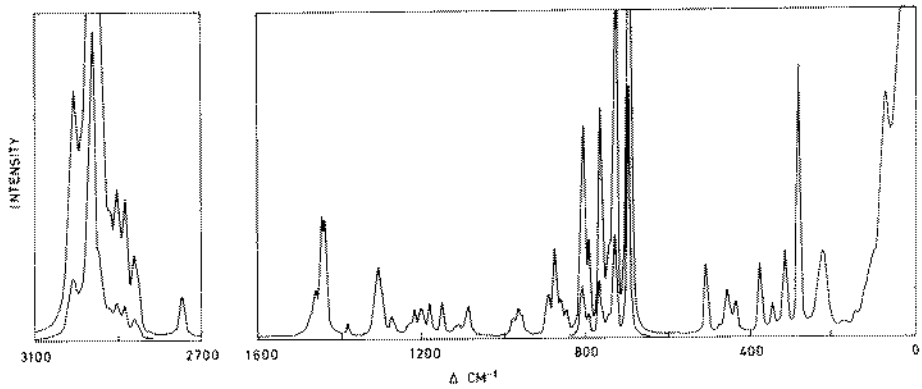

Figure 9. Raman spectrum of TRCN as a liquid.

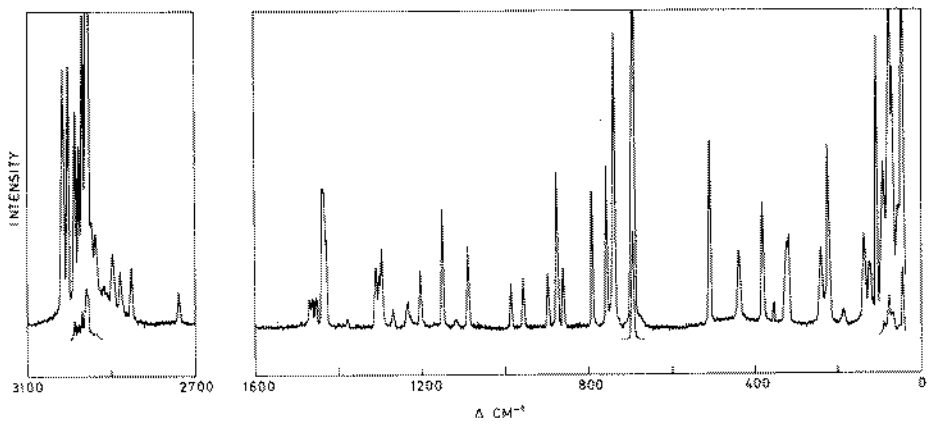

Figure 10. Raman spectrum of TRCN as an annealed, crystalline solid at *ca* 90 K.

Table 1. Vibrational spectral data[a] for 2-(chloromethyl)-2-methyl-1,3-dichloropropane

Infrared			Raman			Interpretation		
Liquid	Solid, 90 K	Solid, 20 kbar	Liquid	depol. ratio	Solid, 90 K	C_1	C_s	C_2
	3016 m[b]				3015 s	ν_1		
	3002 m		3004 s	0.61	3002 s	$\nu_2\nu_3$		
2985 s	2987 s	2994 s	2987 m, sh		2985 s	ν_4		
2976 s	2977 s	2986 s	2978 m, sh		2974 m	ν_5		
	2968 m	2972 m						
2964 s, sh			~2965 s, sh		2967 s	$\nu_6\nu_7$		
	2960 ms	2960 m						
2955 s	2954 ms	2944 w	2957 vs	0.06	2956 vs	ν_8		
~2940 m, sh	2936 w		2942 m, sh		2936 vw			
	2910 w		2918 w	<0.1	2918 vw			
2898 w	2896 w		2899 w	<0.1	2896 w			
2877 w	2878 m	2879 m	2879 w	<0.1	2879 w	ν_9		
2858 w								
2852 w	2852 m	2855 m	2856 w	<0.1	2849 w			
1488 vw			~1485 vw, sh			$\nu_{31}+\nu_{32}$		
1474 m, sh	1472 m	1475 m	1472 w, sh		1472 w	$2\times\nu_{32}$		
1464 s	1461 m	1463 m	1463 w		1464 w	ν_{10}		
1458 s	1455 m	1457 vs	1457 w	0.74	1457 w	ν_{11}		
1442 s	*[c]	*	1442 s	0.73	*		ν_7a'	$\nu_4\nu_{20}a\theta$
	1435 w		1440 m, sh		1440 s	ν_{12}		
1435 s	1433 vs	1433 vs	1435 s	0.75	1435 s, bd	ν_{13}		
1429 s, sh	1428 vs	1429 vs			1432 ms	ν_{14}		
1380 s	1378 vs	1379 vs	1380 w	0.33	1379 vw	ν_{15}		
	1314 w, sh		1312 w, sh		1312 m	ν_{16}		
1304 vs	1307 vs, bd	1304 vs	1304 m	0.60	1306 w	ν_{17}		
1297 vs	1299 vs	1298 s	1298 w, sh		1297 w	ν_{18}		
1273 m	*	*	1272 w		*		$\nu_{12}a'$	ν_7a
	1270 s	1271 s						
1265 m			1265 vw, sh		1269 vw	ν_{19}		
	1266 s	1268 s						
1233 m	1233 s	1236 m	1232 vw		1235 w	ν_{20}		
1228 w, sh					1227 vw			
1218 m	*	*	1218 w	0.72	*		$\nu_{33}a''$	$\nu_{22}e$
1200 w, bd	1203 w	1206 m	1204 w	0.72	1204 w	ν_{21}		
	1192 vw		1196 vw, sh		*		$\nu_{34}a''$	
1180 vw	*	*	1181 w	0.52	*		$\nu_{13}a'$	
1164 vw	1169 m	1170 m			1167 vw			
1150 w	1150 m	1150 m	1150 w	0.52	1151 m	ν_{22}		
	1126 w							
1120 vw, sh	1120 w	1126 w	1120 vw		1117 vw	ν_{23}		
1114 w	*	*	1115 vw		*		$\nu_{23}e$	
1107 w	*	*	1109 vw		*		$\nu_{35}a''$	
1091 w	1089 w		1094 vw, sh					
1085 w	1087 w	1088 w	1086 w		1088 m	ν_{24}		
1035 vw	1038 w	1038 m						
	1016 vw		1015 vw?					
1013 vw	1013 vw							
1001 vw								
997 vw	*	*	993 vw		*		Comb.	
977 m	984 s	988 s	977 w		984 w	ν_{25}		
965 m	*	*	963 w		*		$\nu_{15}\nu_{36}a'a''$	$\nu_{24}e$
957 m	958 s	962 s	957 w	0.65	954 w	ν_{26}		
939 vw	937 w	939 w						
931 w	928 vw							
~895 m, sh	896 vs	898 vs			896 m	ν_{27}		
889 s	*	*	890 m	0.73	*		$\nu_{37}a''$	$\nu_{25}e$
874 s	875 vs	879 vs	874 m	0.54	875 s	ν_{28}		
859 s	858 vs	862 vs	860 w	0.54	859 w	ν_{29}		
846 s	*	*	846 w	0.66	*		$\nu_{38}a''$	
804 w	*	*	806 s	0.25	*		$\nu_{17}a'$	
800 vw, sh								
791 m	789 s	793 s	792 m	0.38	790 s	ν_{30}		
~765 s, sh	*	*	763 s	0.27	*		$\nu_{18}a'$	$\nu_{10}a$
760 vs	756 vs	759 vs	757 m, sh		756 s	ν_{31}		
742 vs	739 vs	739 vs	739 m	0.58	739 s	ν_{32}		

Table 1 (continued)

Infrared			Raman			Interpretation		
Liquid	Solid, 90 K	Solid, 20 kbar	Liquid	depol. ratio	Solid, 90 K	C_1	C_s	C_2
727 m	*	*	728 vs	0.08	*		$\nu_{13}a'$	
704 vs	*	*	706 w, sh		*		$\nu_{39}a''$	$\nu_{11}a$
~695 vs	694 vs	696 vs	696 vs	0.07	693 vs	ν_{33}		
685 vw	687 vw		685 w, sh					
664 vw	660 w		664 vw					
518 m	*	*					$\nu_{40}a''$	
507 s	507 vs	516 vs	508 m	0.45	509 s	ν_{34}		
496 vw	494 vw					$\nu_{36}+\nu_{43}$		
475 w	*	477 vw	476 vw	0.67	*			$\nu_{27}a$
456 vw	*	*	457 w	0.19	*		$\nu_{20}a'$	
436 m	436 m	441 w	437 w	0.49	436 m	ν_{35}		
425 vw	425 vw	415 vw						
378 m	378 m	382 m	378 m	0.20	380 m	ν_{36}		
345 m	*	*	346 w	0.47	*		$\nu_{21}a'$	
	327 m	338 m	322 w, sh		322 w	ν_{37}		
318 s								
	320 s	328 m	316 m	0.20	316 m	ν_{38}		
281 m	*	*	283 s	0.11	*		$\nu_{22}a'$	
261 m	*	260 m	~260 vw				$\nu_{42}a''$	
	239 s							
230 vs		233 m	~230 w, bd, sh		236 w	$\nu_{39}\nu_{40}$		
	230 w							
			221 m	<0.4	221 s	ν_{41}		
		201 w?						
173 w	184 w		173 vw		180 vw	ν_{42}		
145 m	*	147 s	145 vw	<0.5	*		$\nu_{24}a'$	
122 m	136 m	134 w	123 vw		133 w	ν_{43}		
102 m	122 m	111 w	103 vw		118 w	ν_{44}		
	85 w				84 m	l.m.		
71 w			72 m	0.70	70 w	ν_{45}		
					60 m	l.m.		
					45 m	l.m.		

[a] Bands in the regions 5000–3100 and 2800–1500 cm^{-1} have been omitted.
[b] Abbreviations: s, strong; m, medium; w, weak; v, very; sh, shoulder; l.m., lattice mode; bd, broad; FR, Fermi resonance.
[c] Asterisks denotes bands which decrease in intensity with increasing temperature and which disappear in the anisotropic crystal spectra.

Low-temperature behaviour

When the sample was distilled on to the CsI window of the IR cryostat or the copper finger of the Raman cryostat, both held at *ca* 80 K, the spectra obtained were similar to those of the liquid (for IR spectra see the solid curves in Figs 3 and 4). The solid deposits looked transparent by visual observation and apparently consisted of an amorphous glass containing different conformers like the liquid.

The sample was heated very slowly and the IR spectrum recorded at 10 K intervals. At approximately 110 K it was observed that the IR bands marked with asterisks in Table 1 started to increase in intensity relative to the other bands. This effect was accelerated by heating to 120 and 130 K, when the sample still appeared glassy and transparent. Apparently, the conformational equilibria of the vapour at ambient temperature were trapped on the cold window at 80 K, showing up in the spectral intensities. By heating to 110–130 K, the molecules could pass the barriers and adopt the conformational equilibrium for the supercooled liquid at this temperature. Further annealing to *ca* 130–140 K made the sample turn snowy white from an incipient crystallization. Now the reverse process took place in the spectrum and the bands with asterisks diminished and gradually disappeared completely. The remaining bands were frequently shifted, sometimes split into two or more close lines and they had smaller band widths (see Figs 3–5). As is apparent from the Figures and Table 1, the same bands vanished after annealing as those which disappeared in the high-pressure anisotropic phase. Undoubtedly, the same conformer of TRCN was present in both the high-pressure and the low-temperature crystals.

Independent low-temperature spectra were recorded for a sample which was gradually cooled from ambient temperature. For experimental reasons these experiments were performed by the Raman technique only. The liquid was loaded into a capillary tube of 2 mm i.d., placed inside a Dewar vessel and cooled (or heated) by gaseous nitrogen. At 289 K the liquid crystallized to what apparently was a plastically crystalline phase having a Raman spectrum similar to that of the liquid. No lattice modes could be seen in the Raman spectrum (400–20 cm^{-1}) of this phase.

At 253 K a reversible phase transition took place, as is apparent from the disappearance of the Raman bands marked with asterisks in Table 1 and the appearance of

Table 2. Raman intensity data and ΔH^0 between the C_1 and C_s conformers of 2-(chloromethyl)-2-methyl-1,3-dichloropropane (TRCN)

	Plastic phase			Liquid		
Raman band pairs[a]	Intensity[b] (258 K)	Intensity[b] (284 K)	ΔH^0 (kJ mol^{-1} K^{-1})	Intensity[b] (298 K)	Intensity[b] (347 K)	ΔH^0 (kJ mol^{-1} K^{-1})
693	19.0	19.6	5.0	19.0	17.9	2.5
729*	11.4	9.5		6.85	5.45	
693	19.0	19.6	6.6	19.0	17.9	3.9
763*	8.7	6.7		3.85	2.80	
693	19.0	19.6	5.2	19.0	17.9	2.4
806*	7.9	6.5		4.0	3.2	
693	19.0	19.6	5.7	19.0	17.9	3.0
283*	9.7	7.8		5.2	4.0	
376	4.4	5.3	4.4	4.1	6.5	3.4
347*	3.5	3.5		1.5	1.9	
316	4.6	5.5	3.9	4.6	7.35	3.5
347*	3.5	3.5		1.5	1.90	
1150	2.8	2.9	6.1	13.7	13.2	5.2
1180*	3.4	2.7		11.3	8.1	

[a] Each band pair presumably belongs to a C_1 and a C_s conformer.
[b] The intensities were arbitrary relative peak values.

intense lattice bands below 80 cm^{-1}. No additional phase transitions were detected down to 80 K. The crystal formed at 253 K was the same as that formed by annealing the amorphous solid at 130–140 K and probably the same as the high-pressure anisotropic crystal (see above).

Enthalpy difference (ΔH^0) between the conformers

Raman spectra were recorded at 284 and 258 K, both temperatures within the plastic phase, using the 180° scattering mode. It was observed that the bands with asterisks diminished in intensity relative to the other bands. From the relative intensities of suitable band pairs the standard enthalpy difference, ΔH^0, between the most abundant conformers was estimated from the simple relationship $\ln (I_A/I_B)_T = -\Delta H^0/RT$, which was applied at the temperatures (T) 258 and 284 K; I_A and I_B are the peak intensities of Raman bands belonging to conformers A and B, respectively. The calculations are based on the assumption that the molar scattering coefficients for the I_A and I_B bands do not change with temperature. More severe, however, is the assumption that I_A and I_B bands are 'pure,' belonging only to the A and B conformers, respectively. With three conformers present it is very likely that the third minor conformer may overlap one or both of the bands, making the results uncertain. These results are listed in Table 2. The scatter in the ΔH^0 values derived from different band pairs is probably larger than the experimental uncertainties, suggesting that band overlap contributes to some of the results.

Correspondingly, Raman spectra of the liquid at different temperatures were recorded with the same capillary tube within the Dewar vessel, heated by warm nitrogen gas. The liquid was illuminated 90° to the scattered light, unlike the crystalline sample in which the Raman signal was collected 180° from the direction of the illumination. The liquid was studied at 296 and 354 K and again the Raman band intensities were employed to determine ΔH^0. As is apparent from Table 2, the ΔH^0 values of the liquid are significantly lower than the values obtained in the plastic phase.

Independent investigations were carried out by Braathen and Gatial[23] by the matrix isolation technique. They studied TRCN in argon and nitrogen matrices in a 1:1000 ratio and had nozzle temperatures of 300, 600 and 900 K. The IR spectra of the matrices were observed at *ca* 12 K. The intensities of the IR band pairs, 1271*/1265, 860/847*, 743/729* and 518*/507 cm^{-1} were studied as a function of the deposition temperature. As observed in the liquid and plastic crystalline phases (Table 2), the 'vanishing bands' (marked with asterisks) diminished compared with the 'remaining bands.'

Conformer present in the crystal

As is apparent from the Figures and Table 1, the IR and Raman bands vanishing in the crystal are frequently more intense in the liquid, plastic and amorphous states than the bands which remain. Thus, at least two of the three probable conformers of TRCN (Fig. 11) are abundant under these conditions and it is no trivial matter to decide which conformer remains in the crystal.

It was clear, however, that the conformer present in the crystal was not C_3. This conformer has 15 fundamentals of species a and 15 doubly degenerate modes of species e, both being active in both the IR and Raman. The number of IR and Raman bands considered to be fundamentals exceeds this number by far. While 14 fundamentals ($7a+7e$) are expected below 1000 cm^{-1} from the calculations (see Table 3), more than 20 bands with significant intensities were observed. Also, the Raman polarization data are incompatible with seven

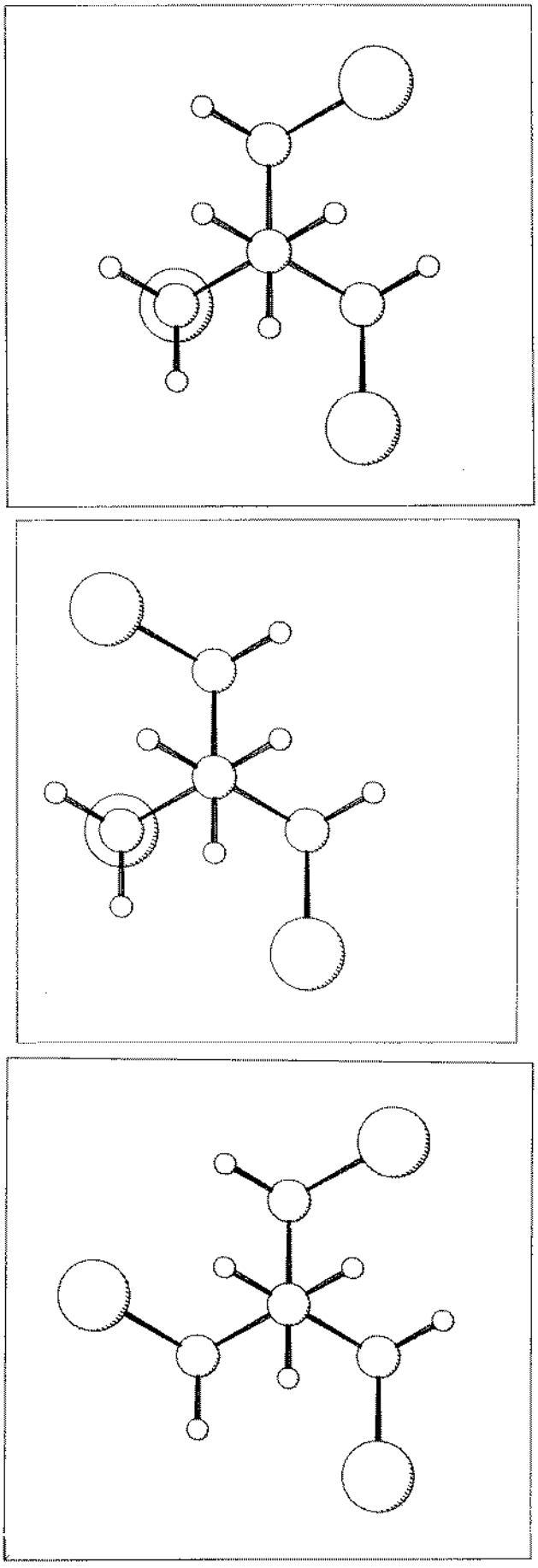

Figure 11. The three TRCN conformers without 1,3-parallel C—Cl bonds and their point groups: C_1 (top), C_s (middle) and C_3 (bottom).

depolarized Raman bands below 1000 cm^{-1} of those remaining in the crystal.

The C_s conformer with *ca* 45% abundance in the vapour at 361 K[11] and 58% in $CBrF_3$ solution at 102 K[14] would *a priori* be considered as the crystal conformer. We would expect 25 polarized Raman bands of species a' and 20 depolarized bands of species a'' of this conformer, which is contradicted by the polarization measurements recorded. Attempts were made to assign the IR and Raman bands of the crystal to the C_s conformer. However, no reasonable agreement with the calculated wavenumbers could be obtained and for the bands calculated at 736, 462, 348, 274 and 211 cm^{-1} of species a' and at 528 and 347 cm^{-1} species a'', the discrepancies between the observed and calculated values were larger than 20 cm^{-1}.

Table 3. Observed and calculated fundamental frequencies for the C_1, C_s and C_3 conformers of 2-(chloromethyl)-2-methyl-1,3-dichloropropane (TRCN)

C_1		C_s		C_3	
Obs.	Calc.	Obs.	Calc.	Obs.	Calc.
3016	3009		3009 (a'')		3008 (a)
3004	3008		3008 (a')		3008 (e)
3004	3007		3006 (a'')		
2985	2967		2967 (a')		2967 (e)
2976	2967		2966 (a'')		
2967	2966		2966 (a')		2966 (a)
2960	2961		2961 (a'')		2961 (e)
2948	2961		2961 (a')		
2870	2883		2883 (a')		2883 (a)
1464	1460		1467 (a')		1464 (e)
1458	1459		1458 (a'')		
1440	1437	1442	1439 (a')	1442	1433 (e)
1435	1435		1437 (a')		
1429	1432		1431 (a'')	1442	1432 (a)
1380	1382		1381 (a')		1386 (a)
1304	1318		1321 (a')		1311 (e)
1304	1311		1313 (a'')		
1298	1293		1294 (a')		1303 (a)
1265	1264	1273	1263 (a')	1273	1275 (a)
1231	1236	1218	1227 (a'')	1218	1222 (e)
1200	1213	1180	1183 (a'')		
1148	1139	1180	1176 (a')	1114	1127 (e)
1120	1118	1107	1113 (a'')		
1084	1080		1077 (a')		1083 (a)
977	966	965	963 (a')	965	965 (e)
957	961	965	962 (a'')		
891	894	889	989 (a'')	889	883 (e)
875	870		866 (a')		
860	864	846	860 (a'')		865 (a)
792	787	806	804 (a')		779 (a)
760	757	763	774 (a')	763	758 (e)
743	750	727	728 (a')		
696	703	704	695 (a'')	704	690 (a)
508	499	518	527 (a'')	475	476 (e)
436	445	456	461 (a')		
378	385	345	349 (a')		380 (a)
318	331	345	348 (a'')		323 (e)
318	314	281	275 (a')		
(230)	251	261	268 (a'')		258 (a)
230	229		242 (a'')		216 (a)
221	210		212 (a')		182 (e)
173	175		184 (a'')		
122	115	145	137 (a')		112 (a)
102	107		82 (a')		98 (e)
71	71		68 (a'')		

A much better agreement between observed and calculated wavenumbers was achieved if it was assumed that the C_1 conformer remained in the crystal (Table 3). Moreover, in the liquid state these bands all appeared polarized, as they should for the C_1 conformer. When the crystal bands were attributed to the C_1 conformer, the vanishing bands could successfully be assigned to C_s and in some cases to the C_3 conformer (Table 3).

Independently, the bands remaining in the crystal were correlated with the thermodynamic stabilities of the conformers. The C_s, C_1 and C_3 conformers have statistical weights 3:6:2, respectively[11]. Simple calculations from the equation $\Delta H^0 = \Delta G^0 + T\Delta S^0$ reveal that the C_s conformer has the lowest ΔH^0 value in the vapour at 361 K[11] and in $CBrF_3$ at 102 K.[14] Since the bands remaining in the crystal are enhanced at increasing temperatures in the vapour,[23] liquid and plastic phases, they must belong to either C_1 or C_3. Only C_1, which is present in a much higher concentration than C_3, is probable. The vanishing bands must accordingly belong to C_s (and/or C_3).

It is surprising that for TRCN it is the second most abundant conformer (C_1) which remains in the anisotropic crystal, rather than the most abundant (C_s). Apparently, the C_1 conformer is favoured in the crystal because of a more favourable lattice energy. Moreover, the C_1 conformer is also present in the high-pressure crystal, unlike the case with 2,2-dimethyl-1,3-dichloropropane.[5] In this compound the C_2 conformer is highly prefered in solution at low temperatures[24] and it crystallizes at low temperature.[5] At high pressure, however, the conformer without symmetry (C_1) is present in the crystal, suggesting a smaller volume for this conformer.[5] It has been suggested[25] that the number of C–X and C–C *gauche* interactions should make a significant contribution to the molar volume. Both in 2,2-dimethyl-1,3-dichloropropane and in TRCN the actual conformers (C_2 and C_1 in the former, C_s, C_1 and C_3 in the latter) have the same number of *gauche* interactions. Therefore, the opposite behaviours of the di- and tri-halogenated neopentanes under high-pressure crystallization indicate that specific atomic contacts in the crystal are deciding the conformer rather than the number of *gauche* interactions.

Spectral interpretation

Based on the IR and Raman spectra, the Raman polarization measurements and particularly the spectral changes that occur on crystallization and with temperature variations, the spectra of TRCN were interpreted. Particularly significant for the spectral assignments were the results of the normal coordinate calculations (see below). The interpretations are listed in Table 1 (experimental data) and Table 3.

Since the C_1 conformer bands remain in the crystal, they are assigned with a great deal of confidence. As is apparent from Table 3, the deviations between the experimental and calculated frequencies were satisfactory. The C_1 bands (fundamentals, overtones and combination bands) were all polarized in the Raman, in agreement with the lack of symmetry for this conformer. All the strong or medium intensity bands were assigned as fundamentals whereas some of the weak lines were interpreted as combinations or overtones.

The bands vanishing in the crystal and decreasing in intensity with increasing temperature were primarily assigned to conformer C_s, since it is known that the C_s abundance is much higher than that for C_3. The high intensities of most of the vanishing bands clearly demonstrate the high concentration of the vanishing conformer(s). While the fundamentals characteristic of the CH_3 and CH_2 stretchings and deformations are common for the three conformers, practically all the a' bands ν_{12}–ν_{24} and a'' bands ν_{33}–ν_{42} appear to be separate for C_s. However, there are no definite criteria by which the C_s bands can be separated from those of C_3. Therefore, the assignments of the bands with asterisks (Table 1) to C_s and/or C_3, mainly based on the force constant calculations, are somewhat arbitrary. It cannot be ruled out that a considerable number of C_1 bands also have contributions from C_s and C_3 in the liquid and plastic phases. As discussed above, the deviations in ΔH^0 calculated from different band pairs suggest that at least some of them are not 'pure' C_1 and C_s. The investigation of TRCN by IR matrix isolation technique[23] might give a clue to overlapping bands because of the narrow bands obtained by this technique.

Normal coordinate calculations

The normal coordinate analysis of the halogenated neopentates was undertaken primarily in order to support the assignments and, in a way, to ensure internal consistency in the interpretations through this series of related molecules: 1-chloro-2,2-dimethylpropane,[4] 1-bromo-2,2-dimethylpropane,[26] 2,2-dimethyl-1,3-dichloropropane,[5] 2-(chloromethyl)-2-methyl-1,3-dichloropropane (TRCN), 2,2-di(chloromethyl)-1,3-dichloropropane[6] and 2,2-di(bromomethyl)-1,3-dibromopropane.[6]

In a previous paper concerning the *trans*-1,4-dihalocyclohexanes[27] we described the advantage of using dimensionless internal stretching coordinates, $\Delta r/r^0$, whereby it is possible to reduce the number of different force constants considerably. The CCX and HCX bending and the torsional force constants are the only parameters that differ for the CH_2Cl and CH_2Br groups in the total of eleven conformer molecules of the halogenated neopentanes mentioned above. We have used, except for the C–halogen distances, common structural parameters for all the compounds. The C–C distances are all set equal to 1.54 Å, the C–H distances to 1.093 Å, the C–Cl and C–Br distances to 1.79 and 1.95 Å, respectively, and all the valence angles are assumed to be tetrahedral.

Apart from the lowest CCX bending modes, all the other normal vibrations throughout the series are reasonably reproduced using a force field transferred from the *n*-alkyl chlorides.[28] The discrepancies for the CCX bending modes are, however, so large and systematic that they cannot be neglected. They are not due to an artifact caused by an incorrect structure or the neglect of an obscure bend–bend interaction constants in the valence force field. Either the CCX bending constants have to be increased from their 'normal' value of *ca* 1 to *ca* 1.5 mdyn Å rad^{-2} or one has to introduce a non-bonded X···H interaction. The first choice implicates

Table 4. Force constants for the halogenated neopentanes

Force mode constant	Group	Coordinate(s) involved	Atoms common to interacting coordinates	Calculated value, ϕ	Standard error, $\sigma\{\phi\}$
Stretch (mdyn Å)					
K_r	CH_3	C—H		5.614	—
K_d	CH_2X	C—H		5.816	—
K_R	C—CH_3	C—C		10.27	0.14
$K_R(X)$	C—CH_2X	C—C		10.40	0.16
K_X	CH_2X	C—X		10.24	—
Bend (mdyn Å rad^{-2})					
H_β	C—CH_3	C—C—H		0.644	—
H_α	C—CH_3	H—C—H		0.534	—
H_γ	C—CH_2X	C—C—H		0.604	0.011
H_δ	C—CH_2X	H—C—H		0.460	0.011
H_θ(Cl)	C—CH_2Cl	Cl—C—H		0.795	0.020
H_θ(Br)	C—CH_2Br	Br—C—H		0.708	0.020
H_ϕ	C—C_3	C—C—C		1.073	0.014
$H_\equiv$(Cl)	C—CH_2Cl	C—C—Cl		0.936	—
$H_\equiv$(Br)	C—CH_2Br	C—C—Br		0.881	—
Torsion (mdyn Å rad^{-2})					
H_τ	C—CH_3	C—C		0.0347	0.0008
H_τ(Cl)	C—CH_2Cl	C—C		0.107	0.005
H_τ(Br)	C—CH_2Br	C—C		0.105	0.009
Stretch–stretch (mdyn Å)					
F_r	CH_3	C—H, C—H	C	0.051	—
F_d(X)	CH_2X	C—H, C—H	C	0.071	—
F_R	C—C_3	C—C, C—C	C	0.46	0.05
F_{RX}	C—CH_2X	C—C, C—X	C	1.17	0.12
Stretch–bend (mdyn Å rad^{-1})					
$F_{R\beta}$	C—CH_3	C—C, C—C—H	C—C	0.329	—
$F_{R\gamma}$	C—CH_2X	C—C, C—C—H	C—C	0.228	0.026
$F_{X\theta}$	C—CH_2X	C—X, X—C—H	C—X	0.87	0.07
$F_{R\equiv}$	C—CH_2X	C—C, C—C—X	C—C	0.46	0.07
$F_{X\equiv}$	C—CH_2X	C—X, C—C—X	C—X	0.98	0.04
$F_{R\phi}$	C—C_3	C—C, C—C—C	C—C	0.73	0.04
Bend–bend (mdyn Å rad^{-1})					
F_β	C—CH_3	C—C—H, C—C—H	C—C	−0.026	—
F_γ	C—CH_2X	C—C—H, C—C—H	C—C	−0.031	0.012
$F_{\gamma\theta}$	C—CH_2X	C—C—H, X—C—H	C—H	0.040	0.005
$F^t_{\gamma\theta}$	C—CH_2X	C—C—H, X—C—H	C	0.029	—
F_ϕ	C—C_3	C—C—C, C—C—C	C—C	0.025	0.010
F_θ	C—CH_2X	X—C—H, X—C—H	C—X	0.126	0.019
$F^t_{\phi\beta}$	C—C—CH_3	C—C—C, C—C—H	(C)—C^{trans}C—(H)	0.049	—
$F^g_{\phi\beta}$	C—C—CH_3	C—C—C, C—C—H	(C)—C^{gauche}C—(H)	−0.052	—
$F^t_{\phi\gamma}$	C—C—CH_2X	C—C—C, C—C—H	(C)—C^{trans}C—(H)	0.049	—
$F^g_{\phi\gamma}$	C—C—CH_2X	C—C—C, C—C—CH	(C)—C^{gauche}C—(H)	−0.052	—
$F^t_{\phi\equiv}$	C—C—CH_2X	C—C—C, C—C—X	(C)—C^{trans}C—(X)	0.034	0.017
$F^g_{\phi\equiv}$	C—C—CH_2X	C—C—C, C—C—X	(C)—C^{gauche}C—(X)	0.037	0.012
Non-bonded interaction (mdyn Å)					
k_{Cl}	CH_2—C—CH_2Cl	Cl···H′		0.403	0.027
K_{Br}	CH_2—C—CH_2Br	Br···H′		0.45	0.05

[a] For definitions of the symbols, see Refs. 28 and 29.

that a number of other force constants also must be changed to 'unusual' values. The second choice may be considered bad taste by 'VFF fanatics,' but it has two advantages in the present case: (1) the strain on the CH_2X groups in the highly branched environment is reflected in a simple way; and (2) the resulting valence force constants are tediously normal. Of the two evils, we prefer the second.

Table 5. Stretch, stretch–stretch and stretch–bend force constants in conventional units

Stretch (mdyn Å^{-1})		Stretch–stretch (mdyn Å^{-1})		Stretch–bend (mdyn rad^{-2})	
K_r	4.531	F_r	0.043	$F_{R\beta}$	0.213
K_d	4.757	F_d	0.059	$F_{R\gamma}$	0.136
K_R	4.330	F_R	0.194	$F_{Cl\theta}$	0.447
$K_R(X)$	4.385	F_{RCl}	0.427	$F_{Br\theta}$	0.339
K_{Cl}	3.231	F_{RBr}	0.390	$F_{R\equiv}$	0.339
K_{Br}	2.693			$F_{Cl\equiv}$	0.581
				$F_{Br\equiv}$	0.553
				$F_{R\theta'}$	0.454

By the least-squares method we have refined a 41-parameter force field to *ca* 280 observed frequencies below 1500 cm^{-1}. In Table 3, the observed and calculated fundamental frequencies for the C_1, C_s and C_3 conformers of TRCN are given, while the corresponding information for 1-chloro-2,2-dimethylpropane[4] and 2,2-di(chloromethyl)1-3-dichloropropane and 2,2-di-(bromomethyl)-2,2-dibromopropane[6] have been given elsewhere. The final force constants are given in Table 4. For the sake of easy comparison with the force constants of other workers, the stretching force constants and the stretch–stretch and stretch–bend interaction force constants are given in Table 5. For definition of the symbols, see Refs 28 and 29.

Acknowledgements

The authors are grateful to Anne Horn for recording some of the spectra. D.L.P. is grateful to the Norwegian Research Council for Science and the Humanities and to the Norwegian Marshall Fund for financial support.

REFERENCES

1. J. Thorbjørnsrud, O. H. Ellestad, P. Klaeboe and T. Torgrimsen, *J. Mol. Struct.* **15**, 45, 61 (1973); J. Thorbjørnsrud, O. H. Ellestad, P. Klaeboe, T. Torgrimsen and D. H. Christensen, *J. Mol. Struct.* **17**, 5 (1973).
2. J. G. Aston and G. H. Messerley, *J. Am. Chem. Soc.* **58**, 2354 (1936).
3. R. Stølevik, *Acta Chem. Scand., Ser. A* **27**, 327 (1974).
4. P. Klaeboe, C. J. Nielsen and D. L. Powell, *Spectrochim. Acta*, Part A **41**, 1315 (1985).
5. D. L. Powell, P. Klaeboe, K. Saebøe and G. A. Crowder, *J. Mol. Struct.* **98**, 55 (1983).
6. P. Klaeboe, B. Klewe, K. Martinsen, C. J. Nielsen, D. L. Powell and D. J. Stubbles, *J. Mol. Struct.*, **140**, 1 (1986).
7. W. H. Urry and J. R. Eiszner, *J. Am. Chem. Soc.* **74**, 5822 (1952).
8. H. B. Thompson and C. C. Sweeney, *J. Phys. Chem.* **64**, 221 (1960).
9. H. Lumbroso, *C.R. Acad. Sci.* **254**, 2750 (1962).
10. H. Lumbroso and D. Lauransan, *Bull. Soc. Chim. Fr.* 513 (1959).
11. R. Stølevik, *Acta Chem. Scand., Ser. A* **28**, 612 (1974).
12. S. Rustad and R. Stølevik, *Acta Chem. Scand., Ser. A* **30**, 209 (1976).
13. R. Stølevik, *Acta Chem. Scand., Ser. A* **28**, 455 (1974).
14. C. H. Bushweller, M. R. Whalon and B. J. Laurenzi, *Tetrahedron Lett.* **22**, 2945 (1981).
15. B. Gilbert and G. Duyckaerts, *Spectrochim. Acta, Part A* **26**, 2197 (1970).
16. F. A. Miller and B. M. Harvey, *Appl. Spectrosc.* **2**, 291 (1970).
17. W. E. Fitzgerald and G. J. Janz, *J. Mol. Spectrosc.*, **1**, 49 (1957).
18. S. D. Christian, J. Grundnes, P. Klaeboe, E. Tørneng and T. Woldbaek, *Acta Chem. Scand., Ser. A* **34**, 391 (1980).
19. P. Klaeboe, J. J. Lothe and K. Lunde, *Acta Chem. Scand.* **10**, 1466 (1956); P. Klaeboe, *Acta Chem. Scand.* **23**, 2641 (1969).
20. T. Woldbaek, *Acta Chem. Scand., Ser. A* **36**, 641 (1982).
21. T. Woldbaek, A. Berkessel, A. Horn and P. Klaeboe, *Acta Chem. Scand., Ser. A* **36**, 719 (1982).
22. C. E. Sjøgren and P. Klaeboe, *J. Mol. Struct.* **100**, 433 (1983).
23. G. O. Braathen and A. Gatial, to be published.
24. M. R. Whalon, G. L. Grady, P. McGoff, R. D. Domingue and C. H. Bushweller, *Tetrahedron Lett.* **23**, 5247 (1982).
25. F. Shahidi, P. G. Farrell and J. T. Edward, *J. Phys. Chem.* **83**, 419 (1979).
26. G. A. Crowder, C. Harper and H.-R. Jalilian, *J. Mol. Struct.* **49**, 403 (1978).
27. T. Woldbaek, C. J. Nielsen and P. Klaeboe, *J. Mol. Struct.* **66**, 31 (1980).
28. R. G. Snyder and J. H. Schachtschneider, *J. Mol. Spectrosc.*, **30**, 290 (1969).
29. R. G. Snyder and J. H. Schachtschneider, *Spectrochim. Acta* **21**, 169 (1965).